

# Electrospinning of epoxy fibers: Effect of curing conditions on solution rheological behavior

Mark Shneider  | Rotem Zattelman | Antonia Kaestner | Israel Greenfeld | Hanoch Daniel Wagner

Department of Molecular Chemistry and Materials Science, Weizmann Institute of Science, Rehovot, Israel

## Correspondence

Hanoch Daniel Wagner, Department of Molecular Chemistry and Materials Science, Weizmann Institute of Science, 7610001 Rehovot, Israel.

Email: [daniel.wagner@weizmann.ac.il](mailto:daniel.wagner@weizmann.ac.il)

## Funding information

Israel Science Foundation, Grant/Award Number: grant #2439/19; Perlman Family Foundation

## Abstract

The electrospinning of thermoplastic polymers is widely used in applications such as filters and coatings, but has only recently been applied to thermosetting polymers because of their chemical structure and reactivity. Epoxy is a thermosetting polymer which, when combined with a curing agent, chemically reacts to form a crosslinked matrix. In the present study, we demonstrate that to electrospin epoxy and obtain continuous micro and nanofibers, one must precisely control the curing reaction. Epoxy was mixed with triamine curing agent and, to enable electrospinnability, was dissolved in a mixture of tetrahydrofuran and dimethylformamide solvents. We identified a narrow working window wherein a proper solution for electrospinning is close to the gel point, right before the transition from liquid to solid gel state. The solution was characterized by means of (i) Fourier-transform infrared spectroscopy to monitor the extent of reaction, (ii) steady shear viscosity to detect the divergence near the gel point, and (iii) oscillatory loss and storage shear moduli to identify the liquid-to-gel transition. Based on these measurements, it was possible to monitor the chemical transformations that the epoxy solution underwent with time, such as chemical interconnections and gelation, and thus define the working window for electrospinning.

## KEYWORDS

crosslinking, electrospinning, epoxy, rheology, thermoset, viscosity

## 1 | INTRODUCTION

Electrospinning (ES) has become a popular fiber production technique for diverse applications, such as filtering and coating.<sup>1</sup> ES is usually used as a fiber preparation technique that processes solutions of thermoplastic polymers of medium molecular weight, dispersed in a dielectric solvent. When such a solution is injected and subjected to a strong electric field, it tends to form a jet, which after solvent evaporation, results in the formation of a thin micro/nanoscale fiber.<sup>2</sup> The primary mechanism for

achieving a continuous fiber as a result of the spinning process in thermoplastics is the molecular entanglement between polymer chains.<sup>3,4</sup>

Epoxy, classified as a thermosetting polymer, exhibits notable advantages over thermoplastic polymers, primarily attributable to its chemically crosslinked structure and its compatibility with various curing agents, leading to superior mechanical properties and exceptional chemical and thermal stability.<sup>5</sup> The crosslinked matrix enables the material to undergo swelling upon exposure to solvents without dissolution, while heating causes softening

without melting. Consequently, epoxy fibers may play a pivotal role in applications where thermoplastic fibers prove unstable, particularly in industries that require chemical and thermal stability, such as filtration, coatings, and polymer composites.

Recently, two groups confirmed the feasibility of ES with a solution of epoxy, a thermoset polymer with low molecular weight. First, Agarwal et al. demonstrated ES of an epoxy dispersion containing carbon nanotubes (CNT).<sup>6</sup> Modulus measurements were performed on a mat of fibers using the atomic force microscopy (AFM) cantilever deflection method, revealing an increase in elastic modulus with increasing CNT volume fraction. Then, Shneider et al. electrospun neat-epoxy microfibers and performed single-fiber tensile measurements, showing plastic deformation of 109% and tensile strength of 121 MPa, comparatively much higher than the known brittle characteristics of bulk epoxy.<sup>7</sup> In both studies, the epoxy resin was dissolved in solvents to make it electrically conductive for ES, and to stabilize fiber formation by fast solvent evaporation.

Epoxy is a crosslinking polymer that forms molecular clusters with time, a process known as curing. The curing reaction is described by Enns and Gillham and expressed by the time–temperature–transformation (TTT) diagram, which shows the various transformation stages the epoxy undergoes during the crosslinking reaction.<sup>8</sup> The reaction starts when epoxy is mixed with a curing agent (hardener), and epoxy monomers progressively bond with each other via the hardener molecules. Gradually, with time and temperature, the density of crosslinking bonds and consequently the solution viscosity increase until the gel point (GP) is reached, when at least one cluster percolates through the entire solution.

Identifying the GP is essential in processing thermoset polymers, because shaping has to occur before the GP while the polymer is still fluid. Therefore, accurate determination of the GP is necessary to enable better processing control. The gel point of a chemically crosslinking system may be defined as the instant at which the polymer's molecular weight diverges to infinity. As a consequence, the polymer undergoes a transition from liquid state to solid state. This phenomenon is called chemical gelation to distinguish it from physical gelation, in which the network is formed by reversible association mechanisms, as in thermoplastic polymers.<sup>9</sup>

The liquid to solid transition during gelation occurs at a critical reaction time  $t_c$ , or equivalently at a critical extent of reaction,  $p_c$ , which depend on the molecular structure of the chemical constituents. For model networks,  $p_c$  is predicted by the bonding functionality and stoichiometric ratio of the constituents.<sup>10–12</sup> These predictions have been found to be in close agreement with

experiments despite differences between molecules of ideal networks and real polymer samples.<sup>9</sup> This suggests that the GP can be detected by monitoring the extent of reaction, tracking it all the way up to the theoretical  $p_c$  value. The most common rheological tests for detecting the GP measure the appearance of an equilibrium modulus or the divergence of the steady shear viscosity. Critical gels (gels near the GP) exhibit a simple and regular relaxation behavior, which expresses itself in a relaxation modulus that was experimentally observed by Winter and Chambon.<sup>13</sup>

ES of epoxy has scarcely been studied, and therefore little is known about the chemical state of the solution and the resulting formation of a continuous ES process. In this study, the ES processing of an epoxy solution is demonstrated, and an analysis of the solution at different curing times is performed. Fourier Transform Infra-Red Spectroscopy (FTIR) analysis, rheological measurements, and ES process tuning are carried out to assess the extent of reaction and to spot and modulate critical areas during the curing reaction. The rheological measurements encompass steady shear viscosity and oscillatory loss and storage moduli using a cone-plate rheometer. These measurements, and the ES of solutions at various curing times, enable us to gain insight into the solution molecular state and the mechanisms that take part in the formation of a continuous fiber by ES.

## 2 | MATERIALS AND METHODS

### 2.1 | Materials

The epoxy used in this study was diglycidyl ether of bisphenol-A (DGEBA), resin EP828 (molecular weight of 340 g/mol) and hardener EP304 (purchased from PolymerG, Israel); the hardener was a polyether amine with trifunctional primary amine. The solvents used were *N,N*-dimethylformamide (DMF) (Sigma-Aldrich) and tetrahydrofuran (THF) (Sigma-Aldrich).

### 2.2 | Solution preparation

The resin and hardener were added in a weight ratio of 100:42 into a glass vial, the same ratio as in previous studies on epoxy fibers for better comparison between the various methods.<sup>7,14</sup> The DMF solvent was used to form an electrically conductive solution, whereas the THF, which is a volatile solvent, evaporated during spinning for faster solidification of the fiber. The solvents were mixed in a weight ratio of 2:8, then added to the

epoxy with a weight fraction of 80% of the total solution weight. The vial was vigorously stirred for 20 min by means of a conditioning mixer (THINKY series ARE-250), then divided into 10 bottles and inserted into the oven for a maximum of 300 h. Ideally, in order to reduce the preparation time, it is possible to increase the temperature for curing, but, for safety reasons, the curing was carried out at 55°C, a temperature lower than the boiling point of THF (65°C). A bottle was removed and frozen at -18°C every few hours at known time points, allowing the curing reaction rate to be inhibited. Prior to any analysis, solutions frozen at the same time point were brought to room temperature while magnetically stirred at 300 rpm for 15 min.

## 2.3 | Spectroscopy

Attenuated total reflection (ATR) FTIR spectroscopy was performed by using a FTIR Alpha (Bruker, UK) equipped with a Platinum ATR. Each sample was tested 2–4 times. A solution of THF/DMF with weight ratio of 8:2 was prepared and used as background reference for the FTIR measurements. Prior to testing, all the solutions were removed from freezing and allowed to warm up to room temperature, then tested right after using the THF/DMF solution as a background, to avoid substantial curing and solvent evaporation. The background solution made it possible to eliminate the solvents absorption peaks and concentrate only on the di-epoxy and the triamine curing agent.

## 2.4 | Rheology

Viscoelastic measurements were performed on a second set of solutions, with a Discovery HR-2 hybrid rheometer (TA Instruments) equipped with a cone plate geometry of 40 mm in diameter and cone angle of 0.5°. A volume of 200 µL was used for all solutions. Each solution was measured 2–4 times, using fast setups to minimize solvent evaporation effect on the measurements.

Three parameters were measured: shear viscosity, storage modulus,  $G'$ , and loss modulus,  $G''$ . All tests were performed at room temperature (25°C). The conditions for shear viscosity were a constant shear rate of 0.1 rad/s. This particular shearing rate was chosen by an experimental optimization procedure, achieving stable results by overcoming the volatile properties of the solution, which tends to evaporate at the cone plate edges.  $G''$  and  $G'$  were measured at an angular frequency sweep range of 10–500 rad/s and strain amplitude of 2%.

## 2.5 | Electrospinning

The homemade electrospinning system (Figure 1a) consisted of a syringe pump (Fusion 4000, Chemyx Inc.) and a DC power supply (PS/FC50R02, Glassman High Voltage, High Bridge, NJ). The nozzle was a needle with inner diameter of 0.83 mm (21 gauge) connected to a disposable syringe. The fiber collector consisted of an aluminum net with a 10 × 10 mm<sup>2</sup> cell size, positioned 150 mm away from the nozzle. A power supply unit was connected to a copper rod electrode 100 mm in length and 2 mm in diameter, located 10 mm behind the net. In this particular setup, the solution extracted from the nozzle is grounded, and attracted by the electric potential of the positively charged copper rod. Upon exiting the nozzle, the solution jet is directed and stretched by the electric field, and flies toward the copper electrode, but is captured by and deposited on the aluminum net which is positioned before the copper electrode (Figure 1). The advantage of this setup lies in its ability to control both the direction and shape of the jet trajectory, which are determined by the type and shape of the electrode and its location with respect to the net.<sup>7</sup> The ES process was carried out at room temperature, using a solution feeding rate of 0.5 mL/h and applied voltage of 19–21 kV for a duration of 10 s, to achieve a low density fiber mesh. The desired ES jet conditions were obtained by varying the feed rate and voltage until fibers without beads were formed. Fibers in a diameter range of 0.15–3 µm and average of 2.39 ± 0.99 µm were collected on the metallic net, then were left to rest for 16 h and finally vacuumed for another 24 h for further solvent evaporation, then cured in an oven at 100°C for 6 h (Figure 1b) according to the manufacture requirements.

## 3 | RESULTS

### 3.1 | Fractional extent of reaction

The epoxy curing reaction involves two sets of constituent monomers: the triamine curing agent, and epoxy (Figure 2a,b). Each epoxy molecule can bind two triamines, one at each end. The curing agent can theoretically bind up to 6 epoxy monomers (chemical functionality of  $f = 6$ ), one as a primary amine and one as a secondary amine on each of the three arms (Figure 2c, top). However, the actual number of cross-links is smaller due to steric and other restrictions. This raises the question what is the monomeric (repeating) unit in our system, for the purpose of determining the monomer chemical functionality and consequently the theoretical critical extent of reaction. Based on the

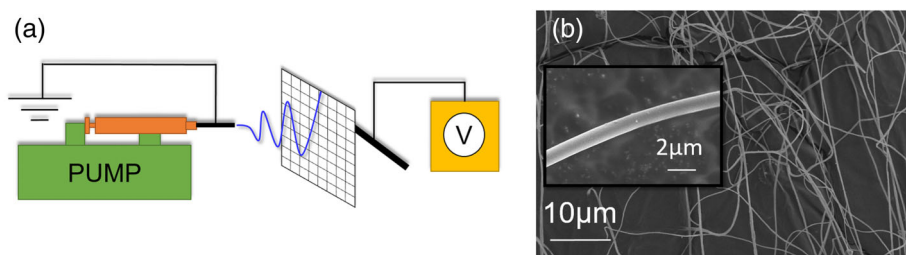


FIGURE 1 (a) Schematic of the electrospinning setup; (b) SEM of typical electrospun fibers. [Color figure can be viewed at [wileyonlinelibrary.com](http://wileyonlinelibrary.com)]

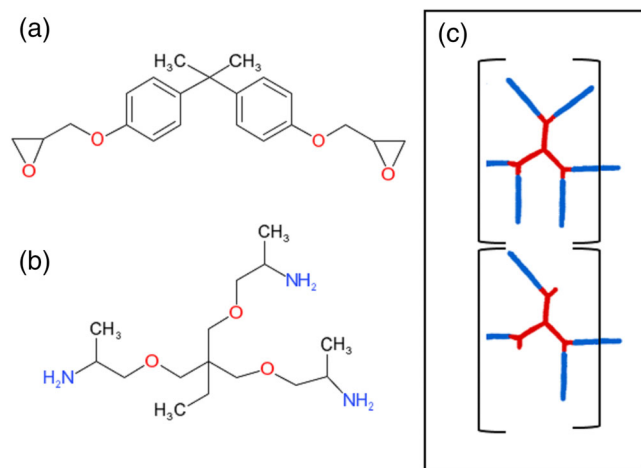


FIGURE 2 (a) Diglycidyl ether of bisphenol-A (DGEBA) epoxy resin EP828 and (b) hardener EP304. (c) Six epoxy monomers (blue) bonded to a curing agent monomer (red) (top,  $f = 6$ ), and four epoxy monomers bonded to a curing agent monomer based on the mol ratio of 3:1 (bottom,  $f = 4$ ). The repeating units are marked by brackets. [Color figure can be viewed at [wileyonlinelibrary.com](http://wileyonlinelibrary.com)]

weight ratio of 100:42 of epoxy ( $m_E$ ) and curing agent ( $m_{CA}$ ) in the solution<sup>7</sup> and the respective molar masses ( $Mw_E = 340$  g/mol and  $Mw_{CA} = 439$  g/mol), the molar ratio is  $\frac{m_E/Mw_E}{m_{CA}/Mw_{CA}} = (100/340)/(42/439) = 3.07$ , close to a ratio of three epoxy monomers to one triamine monomer. This ratio is based on the assumption that at the end of the curing process there is no excess or shortage of curing agent in the solution, in other words, that the solution is a stoichiometric mixture. Thus, each triamine connects on average to 4 epoxy monomers (Figure 2c, bottom), and therefore the actual average functionality of the system is  $f \cong 4$ . The repeating unit is indicated in the figure, showing that each triamine connects on average to three epoxy monomers within the unit, and to an additional epoxy monomer that belongs to another repeating unit, so that the total number of bonds per a triamine monomer is 4. It is assumed that the epoxy molecules can bind only through the curing agent molecules.

The progress of gelation in a solution system is tracked by the extent of reaction,  $p$ . Before the gelation process starts we have a mixture of unreacted monomers,

denoted by  $p = 0$ . When all possible bonds in the network have been formed, gelation and vitrification are completed and the extent of reaction reaches  $p = 1$ . So,  $p$  specifically describes what fraction of all possible bonds is achieved. At some point during the curing progress, the gelation point is reached, defined as the point at which an infinitely large polymer molecule forms that spans the entire system, called the incipient gel. According to gel theory on bond percolation in a branched polymer,<sup>16</sup> the extent of reaction at the gel point,  $p_c$  (critical extent of reaction), depends on the chemical functionality. For a stoichiometric mixture of bifunctional (epoxy) and trifunctional (triamine) monomers, when the functionality of the branching unit (the triamine) is  $f$ , the critical extent of reaction is given from bond percolation modeling for branched polymers<sup>15,16</sup> as:

$$p_c = \frac{1}{f - 1} \quad (1)$$

$p_c$  marks the transition from finite-size polymer molecules to a mixture of infinite-size and finite-size molecules. In our case,  $f \cong 4$  and therefore the predicted critical extent of reaction is  $p_c \cong 0.33$ .

Estimated values of  $p$  for the solutions used in the ES process can be obtained by measurements. FTIR analysis of solutions of different curing times was used to monitor the crosslinking reaction of the epoxy and the triamine curing agent. The preparation of the epoxy solution for ES requires gradual curing with time until reaching a specific crosslinking ratio for stable and continuous fiber formation during the ES process. The kinetics of the reaction involves varying concentrations of four species: Oxirane ring and primary, secondary, and tertiary amines. Two main wavebands are related to the oxirane ring as presented in Figure 3: the absorption band at  $831\text{ cm}^{-1}$ , associated with a symmetric C—O—C stretch of oxirane group, and at  $915\text{ cm}^{-1}$ , associated with an asymmetric C—O—C stretch of oxirane.<sup>17–19</sup> Analyzing the absorbance at different curing times enables quantifying the fractional extent of reaction  $p$  at each curing time point.

In the present case, we found it preferable to calculate  $p$  from the absorbance height  $h$  at the beginning of the

reaction,  $t_0$ , and at different curing times, directly from the  $831\text{ cm}^{-1}$  ring stretching band, as the absorbance in this band had a clear trend without overlaps with samples from other time laps. The values of  $p$  as a function of the curing time  $t$  were calculated by the following correlation<sup>20</sup>:

$$p(t) = \frac{h(t_0) - h(t)}{h(t_0)} \quad (2)$$

The absorbance  $h(t)$  decreases with curing time because of the opening of the oxirane rings, which indicates the creation of a bond, reflected by the extent of reaction progress. As calculated and presented in Figure 4, the fractional extent of reaction shows an increase in oxirane rings

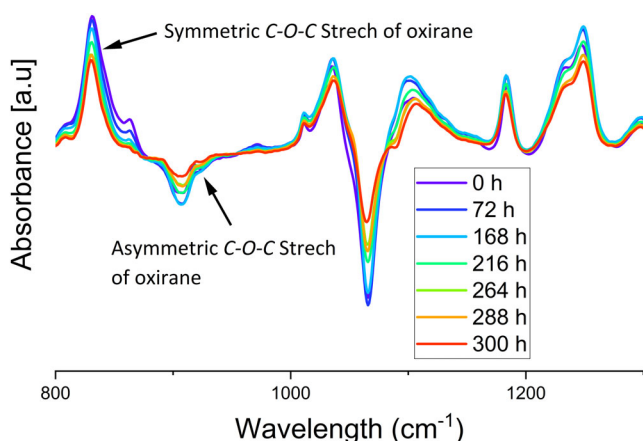
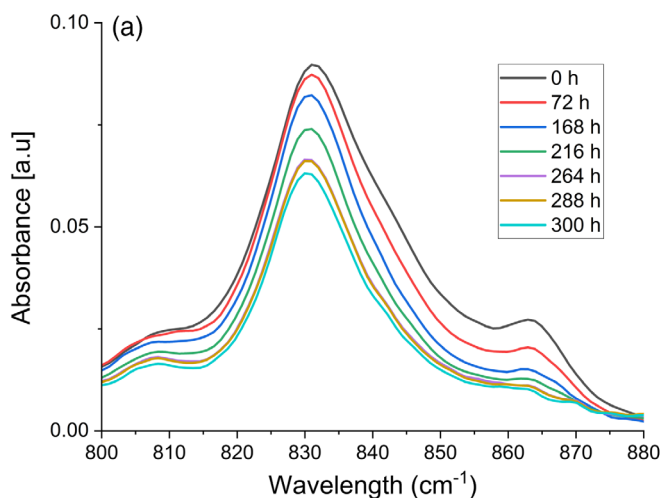


FIGURE 3 FTIR absorbance of epoxy solution at different curing times. [Color figure can be viewed at [wileyonlinelibrary.com](https://onlinelibrary.wiley.com)]



opening up to 30% at 300 h. The solution after 300 h of curing was too viscous for ES but still flowing.

From these results, we can state that the GP should be  $p_c \cong 0.3$  or slightly above it, close to the theoretical prediction (0.33) (Equation (1)), and that it occurs at  $t_c \cong 300$  h or slightly above it. This also implies that the functionality of the system is indeed  $f \cong 4$ , as predicted by the solution stoichiometry. The advantage of evaluating  $p$  in this way is that the curing time for appropriate ES solution can be estimated. We found that the best ES results are achieved in the vicinity of  $p = 0.27$  which occurs at 288 h of curing.

### 3.2 | Storage and loss moduli

Rheological oscillatory shear measurements of storage ( $G'$ ) and loss ( $G''$ ) moduli were performed on solutions at different durations of curing time, as presented in Figure 5.  $G'$  represents the elastic component (stored energy) whereas  $G''$  represents the viscous component (energy loss). The growth in  $G''$  with curing time implies higher viscosity due to the growth of the molecular clusters and the consequent increase in relaxation time. The growth in  $G''$  with increasing  $\omega$  rates reflects the dependence of the dissipation (loss) energy on the dynamic rate. At higher frequencies of 200–500 rad/s, a drop in  $G''$  is observed for all the solutions, possibly due to shear thinning causing a reduction in viscosity at high strain rates. The consolidation in values observed for solutions at curing times longer than 288 h means that the curing time stops affecting  $G''$ , suggesting that the solution approaches the gel state.

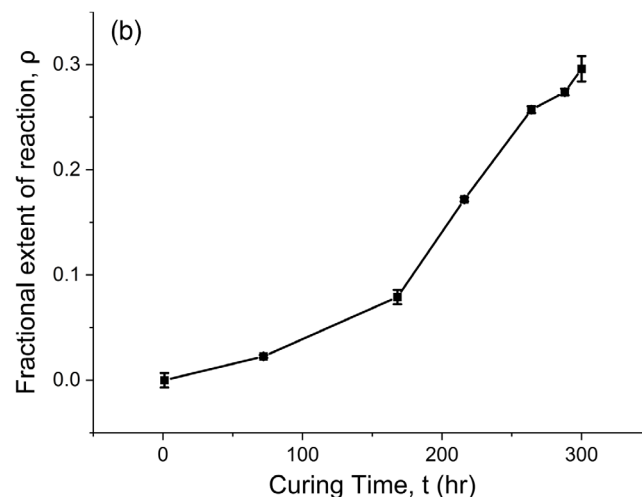
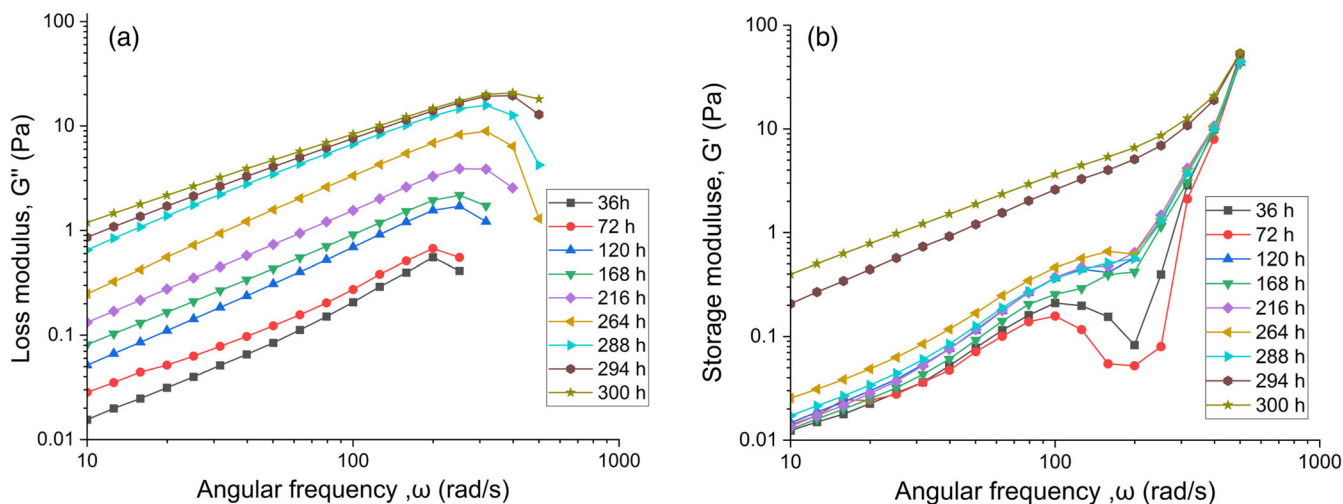


FIGURE 4 Fractional extent of reaction  $p$  versus the curing time  $t$  (b), calculated from FTIR absorbance spectra of symmetric C—O—C bond stretching of oxirane group at wave number  $831\text{ cm}^{-1}$  (a). [Color figure can be viewed at [wileyonlinelibrary.com](https://onlinelibrary.wiley.com)]



**FIGURE 5** Log-Log plots of angular frequency sweep for an epoxy solution at different curing times. (a) Loss modulus ( $G''$ ) and (b) storage modulus ( $G'$ ). [Color figure can be viewed at [wileyonlinelibrary.com](http://wileyonlinelibrary.com)]

The  $G'$  plots presented in Figure 5b also show an increase with  $\omega$ . A gradual increase with consolidation of values for different curing times happens at 50 Pa and 500 rad/s, a result of the high frequency which prevents relaxation from taking place in the solution, regardless of the size of the polymer clusters. The growth in  $G'$  with increasing  $\omega$  rates reflects the dependence of the elastic (storage) energy on the dynamic rate. A reduction in  $G'$  is detected at 200 rad/s, more significant for solutions with lower curing times, whereas solutions at 294–300 h curing do not show any reduction in  $G'$ . As the curing time is decreased, the solutions stop correlating with  $\omega$  within the range of 100–300 rad/s. When the curing time and  $\omega$  are set at these conditions, it appears that the solution is sheared (torn) by the cone-plate rheometer, a condition which gradually disappears when the solution is more viscous and at higher oscillation rate. We also see that for curing times of 294–300 h, the value of  $G'$  jumps abruptly to higher values, signaling a shift in those solutions toward a gel state, characteristic of a largely formed network.

$\tan(\delta)$  is a measure of energy dissipation in the sample and is expressed as the loss to storage moduli ratio,  $\tan(\delta) \equiv G''/G'$ . In this work,  $\tan(\delta)$  is calculated for different curing times at a low-angular frequency of 10 rad/s (Figure 6), providing better sensitivity of the viscous contribution to stress because the solution has more time to relax after stress application.

$\tan(\delta)$  represents the relative measure of the solution's viscous and elastic characteristics: it increases with curing time, indicating that  $G''$  grows faster than  $G'$ . In other words, the viscous effect becomes dominant at longer curing times. By contrast, after 264 h curing, the trend

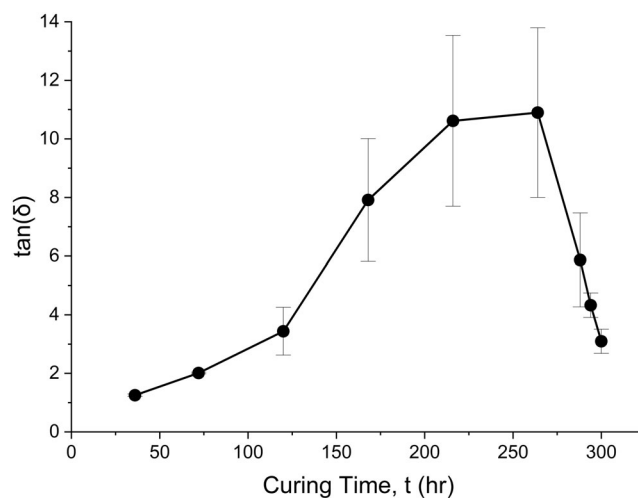
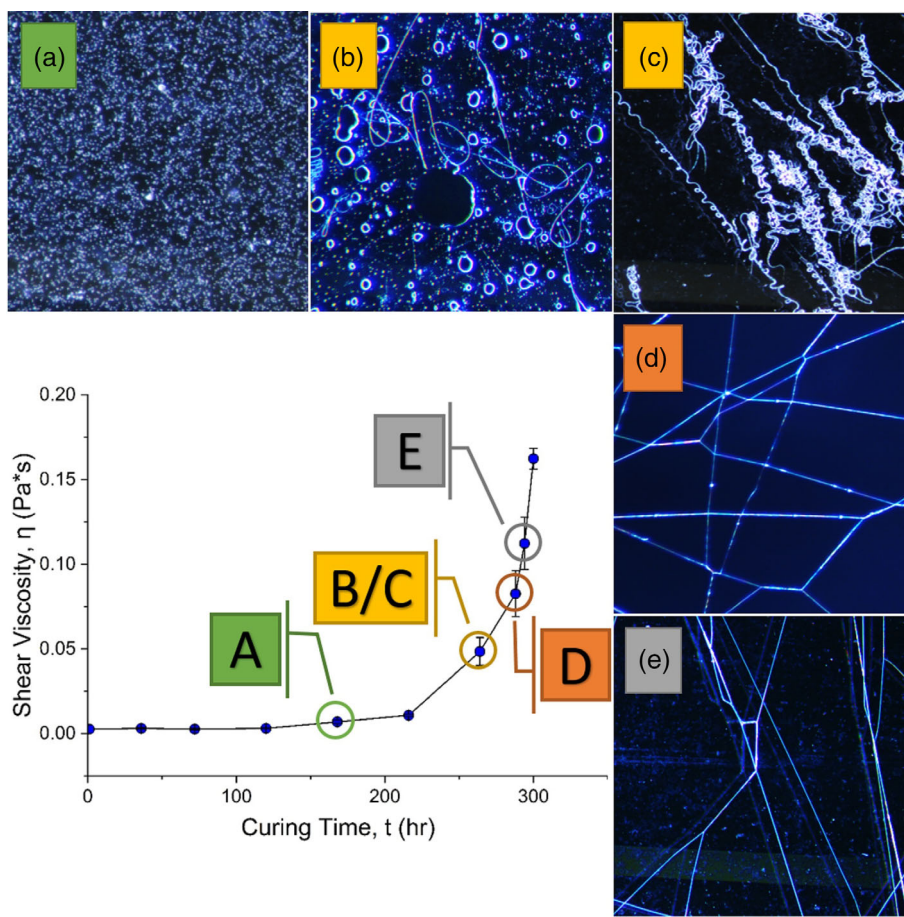


**FIGURE 6**  $\tan(\delta)$  values at different curing times  $t$ , at a constant angular frequency of 10 rad/s.

is reversed, and from then on  $\tan(\delta)$  drops till the end of the test at 300 h. This drop is a clear indication of a sharp increase in  $G'$ , which reflects a rise in elasticity, typical of networks, suggesting that the solution approaches the GP.

We may conclude from the results of  $G'$ ,  $G''$  and  $\tan(\delta)$  that a shift in the mechanical behavior of the solution, particularly as revealed in the trends of  $\tan(\delta)$ , occurs in the curing time range of 264–288 h. A jump in  $G'$  is noted after 294 h, simultaneous with  $G''$  invariance with curing time. For curing times below 264 h, viscosity is dominant, whereas for longer curing times, elasticity is dominant, reflecting the gradual shift from a solution with small polymer clusters to a solution with large, partially overlapping clusters.<sup>16</sup>

**FIGURE 7** Shear viscosity  $\eta$  under constant rate of 0.1 rad/s versus curing time  $t$ . Optical microscope images at  $\times 20$  magnification, after electrospinning of solutions with curing time of (a) 168 h, (b, c) 264 h, (d) 288 h and (e) 294 h. [Color figure can be viewed at [wileyonlinelibrary.com](http://wileyonlinelibrary.com)]



### 3.3 | Shear viscosity

Shear viscosity  $\eta$  was measured by steady shear tests and is presented in Figure 7. At the beginning of the curing process, the solution contains monomers and small polymer clusters with low-molecular weight, resulting in low viscosity. The viscosity then slowly increases up to a curing duration of 216 h, and then starts to grow rapidly until it reaches 0.162 Pa s at 300 h, indicating that the solution gradually approaches the gel point, shifting from an aggregated state to an interconnected state.<sup>16</sup>

Electrospinning of solutions at low curing times up to 264 h, having low viscosity, leads to a formation of electrospinning (small polymer drops) (Figure 7a). For solutions in the 264–288 h curing range, the viscosity increases, and a mixture of large spray drops and fibers appears (Figure 7b,c). At 288 h, only fibers can be seen, some of them also containing beads, but as the curing time reaches 294 h, the beads disappear (Figure 7d). At yet higher viscosities, for solutions cured for more than 300 h, spinning becomes unfeasible.

### 3.4 | Discussion

From the results of solutions at different curing times, two domains are identified at curing times of 0–264 h and 264–300 h, where the 264 h curing time marks the region where transition from beaded to beadless fibers occurs. ES was performed in the 288–294 h range, thus within the second domain. Due to the crosslinking reaction during gel formation, the solution evolves into two stages, namely aggregation and interconnection (or percolation) (Figure 8). During the aggregation stage, epoxy oligomers of low molecular weight tend to combine by crosslinking, forming small clusters that increase in size as the epoxy cures. Consequently, the viscosity increases moderately but remains low at curing times between 0 and 216 h. Using such low-viscosity solutions in the ES process results in electrospinning, the creation of droplets rather than fibers (Figure 7a). As the curing reaction proceeds beyond 216 h, the solution shifts to the interconnection stage (Figure 8c), where larger molecules form and physically interact with their neighbors, as reflected by a steep rise in viscosity. ES with such solutions results in a mixture of spray and short fibers

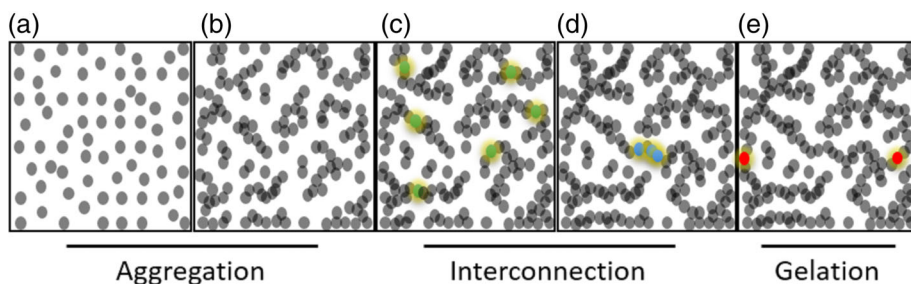


FIGURE 8 Schematic diagram of (a, b) aggregation, (c, d) interconnection and (e) gelation. [Color figure can be viewed at [wileyonlinelibrary.com](http://wileyonlinelibrary.com)]

(Figure 7b,c), the fibers forming only in regions of large molecular clusters, as evidenced by the increase in viscosity. As the clusters grow with curing time, there is less spray until only fibers are formed (Figure 7d). At this point, most of the solution contains large molecules. When an infinitely large molecule spans the entire sample (percolation), gelation is reached and the solution behaves as a solid (Figure 8e).

From the viscosity measurements, we see that continuous fibers can be formed by large molecular clusters when the critical gel point (GP) is approached. To clarify how fibers are formed near the GP, we need to understand the critical gel conditions of the solution. Rheological characteristics near the GP exhibit critical behavior. Both  $G'$  and  $G''$  at the GP can be expressed as<sup>16</sup>:

$$G'(\omega) \sim G''(\omega) \sim \omega^n \quad (3)$$

where  $\omega$  is the angular frequency and  $n$  is the critical relaxation exponent. This power law relation is valid at the GP over a wide range of excitation frequencies and has been widely verified for a variety of polymeric gels.<sup>16</sup> By investigating the relationship between the dynamic moduli and the angular frequency during the isothermal curing process, the GP of the system can be determined accurately.<sup>13</sup> Equation (4) implies a power law time-dependence of the stress relaxation modulus at the GP:

$$G(t) \approx St^{-n} \quad (4)$$

where  $S$  is a temperature-dependent measure of the liquid stiffness or strength.<sup>13</sup> In oscillatory tests, it is possible to convert the modulus from time domain  $G(t)$  to frequency domain  $G(\omega)$ , resulting in the ratio between the loss and storage moduli at the gel point<sup>16</sup>:

$$\tan \delta = \frac{G''(\omega)}{G'(\omega)} \approx \tan\left(\frac{\pi}{2}n\right) \quad (5)$$

For polymers with  $n=1/2$ ,  $\tan \delta=1$  and hence  $G''(\omega)=G'(\omega)$  for a wide range of  $\omega$ .<sup>18</sup> By contrast, in our case, we measured  $\tan \delta \cong 3.1$  (see the end point in Figure 6), which corresponds to a critical relaxation

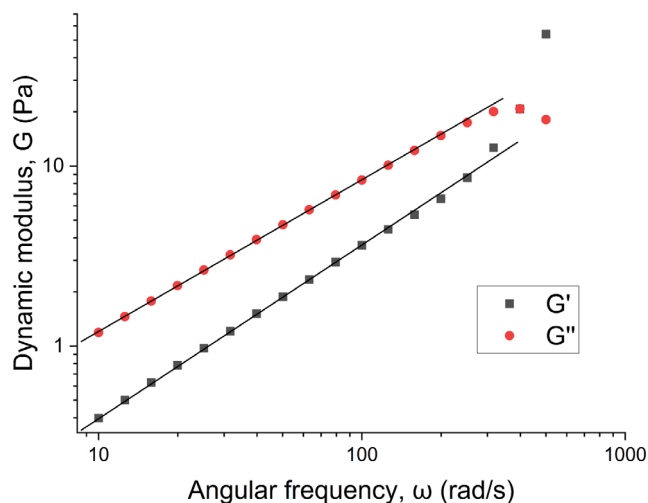


FIGURE 9 Storage modulus  $G'$  and loss modulus  $G''$  power slopes at the gel point, for curing time  $t = 300$  h. [Color figure can be viewed at [wileyonlinelibrary.com](http://wileyonlinelibrary.com)]

exponent of  $n \cong 0.8$  (Equation 5). This can be seen by plotting the dependence of both  $G'$  and  $G''$  versus  $\omega$ , based on the data of Figure 5, and measuring their respective power slopes (see Figure 9). At curing time of 300 h,  $G' \sim \omega^{0.85}$  and  $G'' \sim \omega^{0.96}$ . As at GP the exponent is expected to be the same for both moduli, we may assess that this point is close to GP but slightly below it. Because of the rapid solvent evaporation, it was not possible to get closer to the gel point. The advantage of using the oscillatory shear test over the steady shear test to detect the GP is in avoiding the viscosity divergence in the latter, and in using small amplitudes.

A polymer at GP is characterized by a limiting behavior for both the viscoelastic liquid in the pre-gel region and the viscoelastic solid in the post-gel region. However, a real sample cannot be exactly at the GP. The sample might be arbitrarily close to GP, but it is either still a liquid or already a solid. Such a sample is termed a critical gel or a network polymer at the GP. A solution in the critical gel state can reach gelation with just a few crosslinks holding the gel structure, but when stress is applied, such as the stress induced during the oscillatory tests, it may break these connections and miss the real GP. It

means that when a solution reaches the GP, it may still be fluid when stress is applied. So, we may assume that the GP measured in our experiment is higher compared to the real GP.

Based on the results of  $p$  and according to gelation theory,<sup>16</sup> it is possible to calculate the relative reaction extent  $\varepsilon$  and the characteristic degree of polymerization  $N^*$  when nearing the critical percolation point (GP):

$$\varepsilon \equiv \frac{p}{p_c} - 1 \quad (6)$$

In the pre-gel domain,  $\varepsilon$  ranges from  $-1$  ( $p=0$ ) to  $0$  ( $p=p_c$ ). The degree of polymerization increases with the relative extent of reaction in accordance with a power law derived from percolation theory<sup>16</sup>:

$$N^* \approx |\varepsilon|^{-2.22} \quad (7)$$

As  $|\varepsilon|$  gradually approaches  $0$ ,  $N^*$  diverges, indicating that the solution reached the GP. The viscosity  $\eta$  also increases with the relative reaction extent  $|\varepsilon|$  and follows a power law<sup>16</sup>:

$$\eta \sim |\varepsilon|^{-1.34} \quad (8)$$

We use this relationship to calculate the expected value of  $p_c$  and extrapolate  $t_c$  at the GP. To do so, the  $|\varepsilon|$  values were adjusted by tuning the value of  $p_c$ , so that the viscosity dependence on the relative reaction extent will correspond to a trend line with a power of  $-1.34$  in a log–log plot (Figure 10). A good fit to the theoretical power slope was obtained for a  $p_c$  value of  $0.3075$ , corresponding to  $t_c$  of  $306$  h (extrapolation of the plot in Figure 4b). At these conditions, the solution should turn into a gel.

Integrating the rheological observations, and considering the necessary conditions for achieving continuous fibers during ES of such solutions at a specific curing time, the ES jet is strongly affected by molecular physical and chemical interactions between epoxy clusters. When epoxy solution is approaching the GP with progress in curing time, there is a range in time when the molecular clusters are large enough (represented by the degree of polymerization  $N^*$  in Equation (7) and Figure 10) to form physical interactions such as overlap. In that state, termed hyperscaling, the polymer clusters are at overlap concentration with neighboring clusters, but cannot strongly overlap because that would result in binding and creating a larger cluster.<sup>16</sup> In addition, the interaction between clusters is

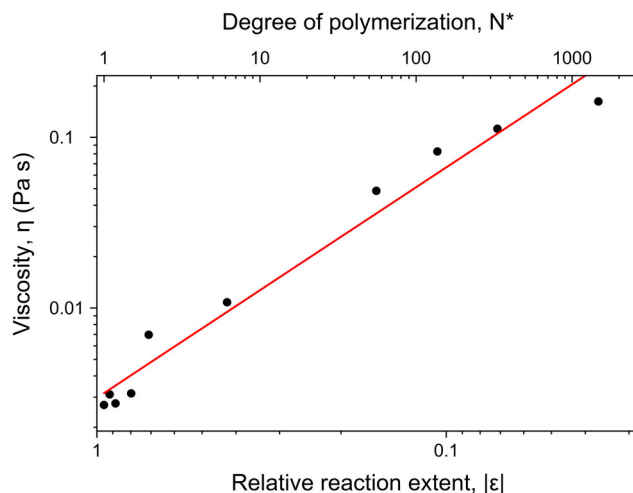


**FIGURE 10** Power law dependence between the measured shear viscosity and the relative reaction extent (reversed axis). Experimental data from Figure 4b and Figure 7. Fitted to a power slope of  $-1.34$  with  $p_c = 0.3075$  (red line). Also shown, the dependence on the degree of polymerization (up to a constant prefactor). [Color figure can be viewed at [wileyonlinelibrary.com](http://wileyonlinelibrary.com)]

enhanced by dipole/hydrogen chemical bonding (Figure 8d).<sup>21</sup> The overlap and chemical interactions play an important role when a solution in that state is used for ES. When the solution surges from the nozzle and is exposed to the electric field, it is strongly stretched and must retain its continuity to create long fibers. The formation of a continuous jet can only occur if there is sufficient interaction between the molecules, otherwise it will break into droplets.

## 4 | CONCLUSIONS

This work describes a rheological analysis of an epoxy solution for electrospinning of micro and nanofibers. The aim was to study the solution's chemical state by means of spectroscopy and rheology, and to specify the state that leads to successful fiber formation. Three main parameters were measured in correlation with curing time: (a) the extent of reaction, (b) the shear viscosity, (c) the dynamic modulus. The analysis of these parameters enabled monitoring of the crosslinking process with dependence on curing time, and calculating the theoretical time to the gel point, consequently identifying a workable region for electrospinning.

It appears that spinning performed with solutions containing large molecular clusters of epoxy in a soluble state is possible. Unlike thermoplastic polymers, in which the entanglement of long polymer chains ensures stable electrospinning and continuous fibers, fiber formation

from a thermoset polymer such as epoxy is likely due to overlaps between clusters, combined with strong dipole and hydrogen chemical bonds. These effects result in a force strong enough to sustain the high shearing generated during electrospinning and form a continuous fiber.

Getting more information on the solution state during electrospinning, and the bulk chemical state after spinning and curing, offers further insights into the crosslinking conditions and morphological state of a vitrified solid epoxy matrix, and better explains the unique mechanical properties of epoxy electrospun fibers. The curing agent was not changed throughout the present study and the effects of varying curing agents will be considered in a future study. Furthermore, ongoing studies aim to investigate the influence of solution curing and electrospinning process parameters on fiber diameter and thermomechanical properties.

#### AUTHOR CONTRIBUTIONS

**Mark Shneider:** Formal analysis (lead); investigation (lead); methodology (lead); visualization (lead); writing – original draft (lead); writing – review and editing (equal).

**Rotem Zattelman:** Investigation (supporting).

**Antonia Kaestner:** Formal analysis (supporting).

**Israel Greenfeld:** Formal analysis (equal); writing – review and editing (supporting).

**Hanoch Daniel Wagner:** Supervision (lead); writing – review and editing (equal).

#### ACKNOWLEDGMENTS

This research was supported in part by the Israel Science Foundation (grant #2439/19), and by the generosity of the Harold Perlman family. H. D. W. is the recipient of the Livio Norzi Professorial Chair in Materials Science. The technical assistance provided by Dr U. Shimanovich and her team at the Weizmann Institute of Science, is greatly acknowledged.

#### DATA AVAILABILITY STATEMENT

The data that support the findings of this study are available from the corresponding author upon reasonable request.

#### ORCID

Mark Shneider  <https://orcid.org/0000-0001-6027-4351>

#### REFERENCES

- [1] X. Xu, H. Lv, M. Zhang, M. Wang, M. Zhou, Y. Liu, D. G. Yu, *Front. Chem. Sci. Eng.* **2023**, *17*, 249.
- [2] J. Xue, T. Wu, Y. Dai, Y. Xia, *Chem. Rev.* **2019**, *119*, 5298.
- [3] I. Greenfeld, X. Sui, H. D. Wagner, *Macromolecules* **2016**, *49*, 6518.
- [4] I. Greenfeld, E. Zussman, *J. Polym. Sci. B Polym. Phys.* **2013**, *51*, 1377.
- [5] P. Mohan, *Polym.-Plast. Technol. Eng.* **2013**, *52*, 107.
- [6] N. Aliahmad, P. K. Biswas, V. Wable, I. Henandez, A. Siegal, H. Dalir, *Appl. Polym. Mater.* **2021**, *3*, 610.
- [7] M. Shneider, X. M. Sui, I. Greenfeld, H. D. Wagner, *Polymer* **2021**, *235*, 124307.
- [8] J. B. Enns, J. K. Gillham, *J. Appl. Polym. Sci.* **1983**, *28*, 2567.
- [9] H. H. Winter, *Polym. Eng. Sci.* **1987**, *27*, 1698.
- [10] P. J. Flory, *Principles of Polymer Chemistry*, Cornell University Press, New York **1953**.
- [11] W. H. Stockmayer, *J. Chem. Phys.* **1943**, *11*, 45.
- [12] C. W. Macosko, D. R. Miller, *Macromolecules* **1976**, *9*, 199.
- [13] H. H. Winter, F. Chambon, *J. Rheol.* **1986**, *30*, 367.
- [14] X. M. Sui, M. Tiwari, I. Greenfeld, R. L. Khalfin, H. Meeuw, B. Fiedler, H. D. Wagner, *Express Polym. Lett.* **2019**, *13*, 993.
- [15] P. J. Flory, *J. Am. Chem. Soc.* **1941**, *63*, 3083.
- [16] M. Rubinstein, R. H. Colby, *Polymer Physics*, Oxford University Press, New York **2003**.
- [17] J. Cañavate, X. Colom, P. Pagès, F. Carrasco, *Polym.-Plast. Technol. Eng.* **2000**, *39*, 937.
- [18] B. C. Smith, *Spectroscopy* **2022**, *37*, 17.
- [19] T. Theophanides, *Infrared Spectroscopy: Materials Science, Engineering and Technology*, BoD–Books on Demand, Rijeka, Croatia **2012**.
- [20] M. Mours, H. H. Winter, *Macromolecules* **1996**, *29*, 7221.
- [21] W. Li, J. Ma, W. Shinan, J. Zhang, J. Cheng, *Polym. Test.* **2021**, *101*, 107275.

**How to cite this article:** M. Shneider, R. Zattelman, A. Kaestner, I. Greenfeld, H. D. Wagner, *J. Appl. Polym. Sci.* **2023**, e54437. <https://doi.org/10.1002/app.54437>